Predicting Some Stand Attributes of Scots Pine Stands Using Landsat 8 OLI Satellite Image

DÖNDÜ DEMİREL[1]*, OYTUN EMRE SAKICI[1], ALKAN GÜNLÜ[2]

Abstract

Monitoring forest resources using satellite images has been employed for different forest inventory purposes. This study used remote sensing data to derive regression models for estimating some stand attributes, including mean diameter, stand basal area, stand volume, number of trees, and stand density of pure Scots pine (*Pinus sylvestris* L.) stands. Field measurements were conducted within the 135 sample plots to obtain the above-mentioned stand attributes data. Reflectance values, vegetation indices, and texture values of each sample plot were generated from Landsat 8 OLI satellite images. The data obtained from sample plots were randomly selected and divided into two groups, consisting of 101 sample plots (75% of total data) for derivation of models, and 34 sample plots (25% of total data) for validation of the derived models. The prediction strengths of seven independent variable groups (i.e., reflectance values, vegetation indices, texture values, reflectance values and vegetation indices, reflectance values and texture values, vegetation indices and texture values, reflectance values, vegetation indices, and texture values) were also compared. A multiple linear regression analysis was utilized to fit stand attributes based on the derived independent variable groups. Three goodness-of-fit statistics (R^2, *RMSE* and *MAE*) were used to compare the different prediction models. Results revealed a moderate success of the derived regression models. Best models for mean diameter, stand basal area and number of trees were achieved with vegetation indices and texture values as independent variable group, with R^2 values of 0.492, 0.338 and 0.534, respectively.

Keywords: *stand parameters, passive sensor, multiple linear regression, Pinus sylvestris*

[1]**Kastamonu University, Faculty of Forestry, 37150, Kastamonu,Türkiye**

[2]**Çankırı Karatekin University, Faculty of Forestry, 18200, Çankırı/ Türkiye**

[1]***Corresponding Author*. Kastamonu University, Faculty of Forestry, 37150, Kastamonu,Türkiye**

E-mail Address: ddemirel@kastamonu.edu.tr

I. INTRODUCTION

Sustainable forest management plans are usually supported by forest inventory data that provides information about the current state of the forest [2]. Data on stand attributes such as mean diameter, stand basal area, stand volume, number of trees and stand density in forest inventory are useful information in the formulation of forest management plans. Although field measurements and observations are the most widely used method in forest inventory, the setbacks of this approach include high costs, labor-intensive, and time-consuming [30]. These limitations could be addressed through employment digital technology in forest inventory in which the forest data can be obtained through remote sensing methods [7, 17]. Remote sensing, which captures images using various satellites such as Landsat, IKONOS, QuickBird, Sentinel, Göktürk, provides important spatial and temporal data for utilization in planning and forest inventory activities [41]. The Landsat 8 OLI satellite, which has been providing data since 2013, have been used in many forestry studies, such as classification of land cover [24], estimation of stand attributes [1, 20], estimation of leaf area index [4, 10] and estimation of aboveground biomass and carbon stock [35, 20, 43, 31, 14].

Many reported studies used reflectance values, vegetation indices, and texture values obtained from Landsat 8 OLI satellite images to determine stand attributes [1, 40, 4, 19, 20, 43, 14]. These studies derived prediction models based on the relationships between stand attributes and remote sensing data, which are used to estimate stand attributes. Most of these models employed multiple linear regression [20], artificial neural networks [40, 35], *k*-nearest neighbor [1], random forest [10], geographically weighted regression [20] and extreme gradient boosting [31] methods to predict or estimate stand attributes.

The purpose of this research is to develop regression models for various stand attributes (mean diameter, stand basal area, stand volume, number of trees and stand density) in pure Scots pine (*Pinus sylvestris* L.) stands of Kösdağ Planning Unit (Kastamonu, Türkiye) using the reflectance values, vegetation indices and texture values obtained from the Landsat 8 OLI satellite

image. The relationships between stand attributes and remote sensing data were investigated using a multiple linear regression method and the effects of different independent variable combinations of reflectance values, vegetation indices and texture values on the prediction success were assessed.

II. MATERIALS AND METHODS

Study Area

This study was conducted in the Scots pine stands in Kösdağ Planning Unit within the boundaries of the Tosya Forest Enterprise, Kastamonu Regional Directorate of Forestry (40° 56' 55" - 41° 03' 45" N, 34° 13' 25" - 34° 24' 17" E). The Kösdağ Planning Unit consists of 6908-ha total forest area in which the Scots pine stands comprise about 35% (2420 ha) of the total area. The slope ranges from 4% to 62%, with an average value of about 27%. The elevation ranges between 1552 to 2051 m with an annual mean temperature and precipitation of about 12.0 °C and 404.6 mm, respectively (Fig. 1).

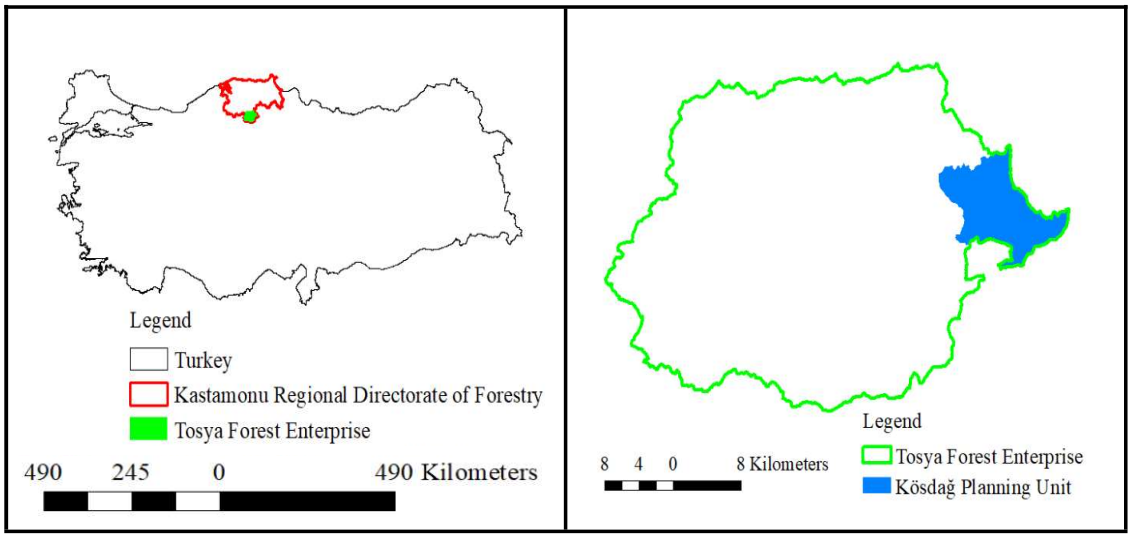

Figure 1. Geographical Location of the Study Site

Measurement Procedure

A total of 135 sample plots of pure Scots pine stands from sample plots, which were used in the forest inventory activities

during the preparation of the Kösdağ Forest Management Plan in 2014, were utilized in this study. The sizes of circular sample plots were 800-, 600- and 400-m², based on the crown closure classes of the stands (i.e., 11 to 40%, 41 to 70%, and >70%). Landsat 8 OLI satellite images of the study area and location of sample plots are shown in Figure 2.

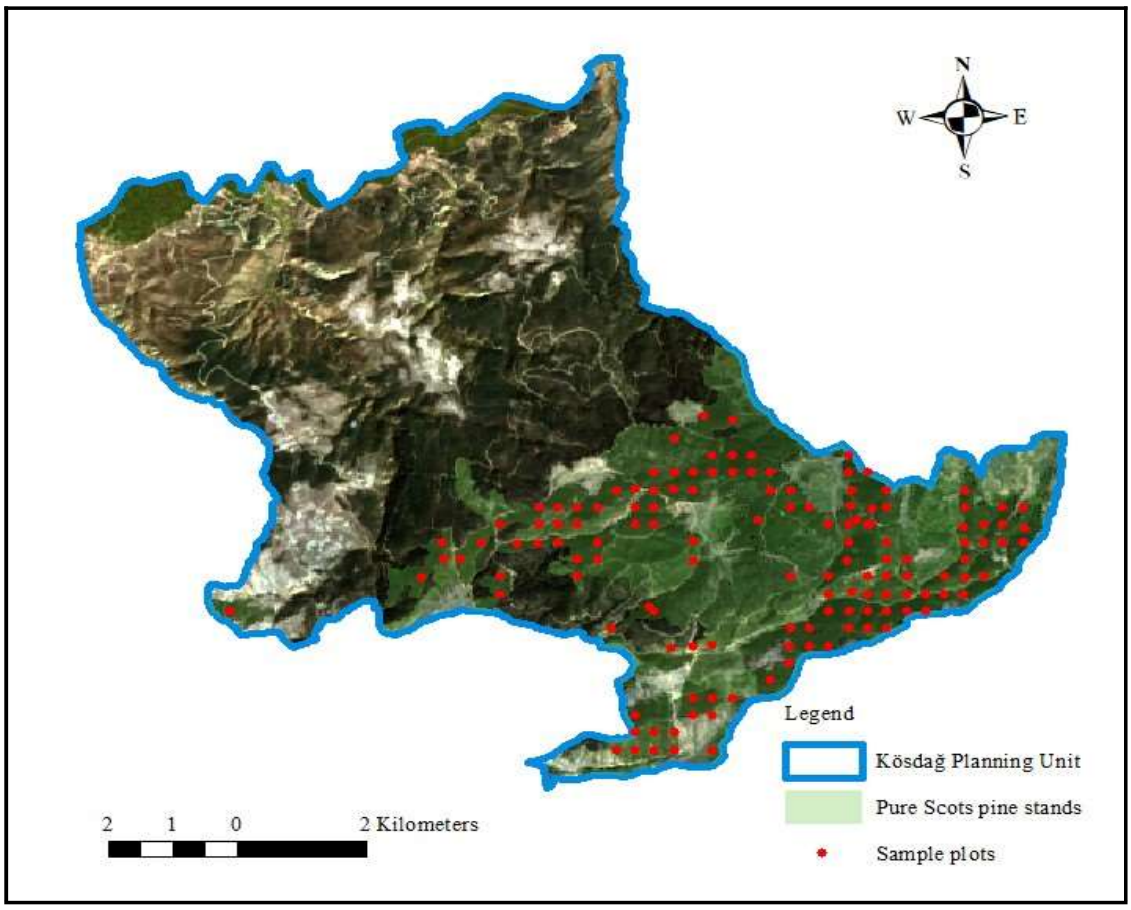

Figure 2. Landsat 8 OLI Satellite Image of Study Area and Location of Sample Plots

The coordinates, centered at each sample plot, were determined with GPS according to the UTM coordinate system. Within these sample plots, the diameter at breast height (dbh, cm) of trees greater than 7.9 cm and number of trees (*n*) were measured. A total of 3,426 trees were measured at dbh in all sampling plots with total number of trees ranging from 5 to 49 for each sampling plot. The basal area and volume of all trees were calculated using the measured dbh. Volume calculations were done using the single-entry volume equation by Yavuz *et al.* [46] (Equation 1). Mean

diameters of sample plots were calculated as quadratic mean diameter (d_q, cm) (Equation 2). Total basal area (g, m^2) and total volume (v, m^3) of sample plots were obtained by adding the basal areas and volumes of sample trees, and then converted to stand basal area (G, $m^2\ ha^{-1}$) and stand volume (V, $m^3\ ha^{-1}$) based on equations 3 and 4. The number of trees (N, trees per ha) was obtained using Equation 5. The stand density (SD) was determined using the equation by Curtis *et al.* [9] (Equation 6) where d_q, mean diameter (cm); dbh, diameter at breast height (cm); G, stand basal area ($m^2\ ha^{-1}$); g, basal area of the sample plot (m^2); V, stand volume ($m^3\ ha^{-1}$); v, volume of the sample plot (m^3); N, number of trees per hectare; n, number of trees in sample plot; and A, sample plot size (m^2).

$$\ln v = -8{,}209 + 2{,}324 \ln dbh - \frac{3{,}664}{dbh} \quad (1)$$

$$d_q = \sqrt{\frac{\sum dbh^2}{n}} \quad (2)$$

$$G = \frac{10000}{A}\, g \quad (3)$$

$$V = \frac{10000}{A}\, v \quad (4)$$

$$N = \frac{10000}{A}\, n \quad (5)$$

$$SD = \frac{G}{\sqrt{d_q}} \quad (6)$$

One hundred thirty-five sample plots were randomly selected and divided into two groups, consisting of 101 sample plots (75% of total sample plots) for the model development and 34 sample plots (25% of total sample plots) for use in the validation process.

Descriptive statistics of the sample plots for model development and validation data groups are summarized in Table 1.

Table 1. Descriptive Statistics of the Sample Plots

Statistics	Mean diameter (cm)	Basal area (m^2 ha^{-1})	Stand volume (m^3 ha^{-1})	Number of trees (per ha)	Stand density
Model development data (101 sample plots)					
Minimum	8.7	4,035	18,764	63	1.37
Maximum	60.8	76,455	821,182	1225	12.84
Mean	29.4	28,518	284,046	480,6	5.18
Standard deviation	10.3	14,810	164,685	252,4	2.38
Validation data (34 sample plots)					
Minimum	10.3	3,463	18,696	138	1.07
Maximum	55.2	48,733	550,032	1150	8.41
Mean	30.6	25,551	259,442	404,4	4.55
Standard deviation	10.6	11,594	137,095	228,3	1.74

Remote Sensing Data and Data Processing

The Landsat 8 OLI satellite image in 2014 was used in this study (http://earthexplorer.usgs.gov) to be consistent with the 2014 field measurements data in this study. The strip width of this image is 185 km with temporal resolution of 16 days. There was no requirement for correction because the Landsat 8 OLI satellite image was obtained in Level-1 C format, which includes atmospheric, radiometric, and geometric corrections. The remote sensing data were divided into three groups as reflectance values, vegetation indices and texture values. The reflectance values were calculated for each sample plot separately for six bands (2, 3, 4, 5, 6 and 7) of the Landsat 8 OLI satellite image with 30-m spatial resolution. The reflectance values of the sample plots were obtained in two stages. In the first stage, each band of Landsat 8 OLI satellite image was calibrated using QGIS Desktop 3.8.1 software, and then obtained the reflectance values of each band. The extraction of the reflectance values of the sample plots was carried out in the second stage using the ArcGIS Desktop 10.5.1 software. A “buffer zone” was delineated on the center of sample plots according to the sample plot sizes (with 11.28, 13.82 and 15.96 m radius), and

then obtained the actual sample plot sizes. Then, reflectance values of each sample plot were obtained by using the "zonal statistics as table" command for each band. The reflectance values were estimated based on the average of the pixel values within the sample plot boundaries. Vegetation indices were calculated based on the 24 different vegetation indices obtained from the literature. The values of six bands of the Landsat 8 OLI satellite image were used in the calculation of these indices (Table 2).

Table 2. Calculated Vegetation Indices

Vegetation indices	Formula	Reference
MID	$Band6 + Band7$	Kaufman & Remer [25]
NDVI	$\frac{Band5 - Band4}{Band5 + Band4}$	Rouse *et al*. [39]
MSI	$\frac{Band6}{Band5}$	Hunt & Rock [17]
NDMI	$\frac{Band5 - Band6}{Band5 + Band6}$	Hardisky *et al*. [16]
NBR	$\frac{Band5 - Band7}{Band5 + Band7}$	Key & Benson [27]
EVI	$2.5\left(\frac{Band5 - Band4}{Band5 + 6Band4 - 7.5Band2 + 1}\right)$	Liu & Huete [29]
SAVI	$1.5\left(\frac{Band5 - Band4}{Band5 + Band4 + 0.5}\right)$	Huete [18]
MSAVI	$\frac{2Band5 + 1 - \sqrt{(2Band5 + 1)^2 - 8(Band5 - Band4)}}{2}$	Qi *et al*. [37]
ARVI	$\frac{Band5 - 2Band4 + Band3}{Band5 + 2Band4 - Band3}$	Kaufman & Tanre [26]
ND32	$\frac{Band4 - Band3}{Band4 + Band3}$	Lu *et al*. [30]
ND53	$\frac{Band6 - Band4}{Band6 + Band4}$	Lu *et al*. [30]
ND73	$\frac{Band7 - Band4}{Band7 + Band4}$	Lu *et al*. [30]

Table 2. (Continued)

Vegetation indices	Formula	Reference
GNDVI	$\frac{Band5 - Band3}{Band5 + Band3}$	Gitelson *et al*. [11]
NDWI	$\frac{Band5 - Band6}{Band5 + Band6}$	McFeeters [32]
MSR	$\left(\frac{Band5}{Band4} - 1\right) \Big/ \left(\sqrt{\frac{Band5}{Band4}} + 1\right)$	Chen [6]
NLI	$\frac{Band5^2 - Band4}{Band5^2 + Band4}$	Goel & Qin [12]
PSSR	$\frac{Band5}{Band4}$	Blackburn [3]
IPVI	$\frac{Band5}{Band5 + Band4}$	Crippen [8]
RVI	$\frac{Band5}{Band4}$	Jordan [22]
EVI2	$2.4\left(\frac{Band5 - Band4}{Band5 + Band4 + 1}\right)$	Jiang *et al*. [21]
DVI	$Band5 - Band4$	Tucker [42]
MID57	$Band5 + Band7$	Lu *et al*. [30]
VIS123	$Band2 + Band3 + Band4$	Lu *et al*. [30]
Albedo	$Band2 + Band3 + Band4 + Band5 + Band6 + Band7$	Lu *et al*. [30]

Table 3. Independent Variable Groups for MLR Models

Independent variable groups*	Variables					Number of variables
R	B2, B3, B4, B5, B6 and B7					6
VI	MID, NDVI, MSI, NDMI, NBR, EVI, SAVI, MSAVI, ARVI, ND32, ND53, ND73, GNDVI, NDWI, MSR, NLI, PSSR, IPVI, RVI, EVI2, DVI, MID57, VISI23 and Albedo					24
T	Bands (6)		Window sizes (4)		Texture metrics (8)	192
	B2, B3, B4, B5, B6, B7	*x*	3x3, 5x5, 7x7, 9x9	*x*	M, VAR, HOM, CONT, DIS, ENT, SM, COR	
R – VI	B2, B3, B4, B5, B6, B7, MID, NDVI, MSI, NDMI, NBR, EVI, SAVI, MSAVI, ARVI, ND32, ND53, ND73, GNDVI, NDWI, MSR, NLI, PSSR, IPVI, RVI, EVI2, DVI, MID57, VISI23 and Albedo					30
R – T	B2, B3, B4, B5, B6, B7 and 192 texture values					198
VI – T	MID, NDVI, MSI, NDMI, NBR, EVI, SAVI, MSAVI, ARVI, ND32, ND53, ND73, GNDVI, NDWI, MSR, NLI, PSSR, IPVI, RVI, EVI2, DVI, MID57, VISI23, Albedo and 192 texture values					216
R – VI – T	B2, B3, B4, B5, B6, B7, MID, NDVI, MSI, NDMI, NBR, EVI, SAVI, MSAVI, ARVI, ND32, ND53, ND73, GNDVI, NDWI, MSR, NLI, PSSR, IPVI, RVI, EVI2, DVI, MID57, VISI23, Albedo and 192 texture values					222

To determine the texture values, the gray level co-occurrence matrix (GLCM) proposed by Haralick *et al*. [15] was used. Eight texture metrics (mean (*M*), variance (*VAR*), homogeneity (*HOM*), contrast (*CONT*), dissimilarity (*DIS*), entropy (*ENT*), second moment (*SM*) and correlation (*COR*)) were generated using four different window sizes (3 x 3, 5 x 5, 7 x 7 and 9 x 9) for 6 bands of Landsat 8 OLI satellite image. Obtaining the texture values of the sample plots was carried out in two stages. First, the texture analysis was performed for each band of Landsat 8 OLI satellite image using ENVI 5.2 software. Second, texture values were obtained for each sample plot by using the "zonal statistics as table" command to the image obtained for each texture metrics with the "buffer zone" by using ArcGIS Desktop 10.5.1. Thus, for each sample plot, a total of 192 texture values were produced, as a combination of 6 different bands, 4 different window sizes and 8 different texture values. The texture values were obtained as the mean values within the sample plot boundaries (buffer zone). As a result, 222 remote sensing data were produced for each sample plot, including 6 reflectance values, 24 vegetation indices and 192 texture values obtained from Landsat 8 OLI satellite image.

Regression Models

Multiple linear regression (MLR) was used to model the relationships between the stand parameters of measured field data (mean diameter, basal area, stand volume, number of trees, and density) and remote sensing data derived from the Landsat 8 OLI satellite image (reflectance values, vegetation indices, and texture values). The ordinary least squares method was used to obtain MLR models based on the stepwise variable selection method. In the regression models, stand attributes of the model data group (101 sample plots) obtained by field measurements were used as the dependent variable. The independent variables are the remote sensing data in three different groups: reflectance values, vegetation indices and texture values obtained from the Landsat 8 OLI satellite image. To develop the regression models, each remote sensing data group was processed independently of each other. Then, the relationships in binary combinations, such as reflec-

tance values-vegetation indices, reflectance values-texture values, and vegetation indices-texture values, were revealed. Finally, reflectance values-vegetation indices-texture values were included in the model together. As a result, seven different models based on different data sets were developed for each stand attributes (Table 3). The individual and mixed effects of reflectance values, vegetation indices and texture values on the prediction success of stand characteristics were also evaluated and assessed. Regression models were fitted using IBM SPSS 23 software.

Model Comparisons and Validation Tests

The multiple linear regression models were compared based on goodness-of-fit statistics involved coefficient of determination (R^2), root mean square error (*RMSE*) and mean absolute error (*MAE*).

$$R^2 = 1 - \frac{\sum(y_i - \hat{y}_i)^2}{\sum(y_i - \bar{y})^2} \quad (7)$$

$$RMSE = \sqrt{\frac{\sum(y_i - \hat{y}_i)^2}{n-1}} \quad (8)$$

$$MAE = \frac{\sum|y_i - \hat{y}_i|}{n} \quad (9)$$

where y_i , observed values of stand attributes; $\hat{y}_i$, predicted values of stand attributes, and *n*, sample size.

To compare the regression models fitted with different independent variable groups for each stand parameter, the relative ranking approach by Poudel & Cao [38] was used. In this approach, the relative rank of each regression model for a goodness-of-fit statistic is determined using Equation 10. Once each model ranked the goodness-of-fit statistics, relative ranks of statistics were summed up and the total relative ranks of regression models were re-ranked to determine the overall ranks.

$$R_i = 1 + \frac{(m-1)(S_i - S_{min})}{(S_{max} - S_{min})} \quad (10)$$

where R_i, relative rank of model i (i=1, 2, ..., m); S_i, goodness-of-fit statistic of model i; S_{min} and S_{max}, minimum and maximum values

Table 4. Multiple Linear Regression Results for Mean Diameter

Independent variable groups	Independent variables (X_i)	Coefficients (b_i)	*p*-value	R^2	*SEE*
R	Constant	94.065	0.000	0.186	9.467
	B2	-910.441	0.042		
	B5	-219.108	0.000		
	B6	275.003	0.003		
VI	Constant	34.336	0.001	0.204	9.311
	EVI	-1358.393	0.004		
	SAVI	1482.370	0.008		
T	Constant	42.254	0.000	0.408	8.112
	B5-3x3-M	-0.307	0.000		
	B5-9x9-HOM	-0.111	0.000		
	B6-3x3-M	0,431	0.000		
	B7-9x9-M	-0,290	0.000		
R – VI	Constant	34.336	0.001	0.204	9.311
	EVI	-1358.393	0.004		
	SAVI	1482.370	0.008		
R – T	Constant	51.603	0.000	0.433	8.026
	B5	-230.333	0.000		
	B6	288.879	0.000		
	B5-5x5-HOM	-0.107	0.010		
	B5-7x7-HOM	0.314	0.001		
	B5-9x9-HOM	-0.329	0.000		
	B7-9x9-M	-0.221	0.000		
VI – T	Constant	59.148	0.000	0.492	7.678
	EVI	-1065.453	0.000		
	EVI2	1167.627	0.000		
	B3-7x7-M	0.387	0.007		
	B4-9x9-DIS	-0.151	0.000		
	B5-5x5-COR	-0.058	0.001		
	B5-9x9-M	-0.408	0.001		
	B5-9x9-HOM	-0.176	0.000		
	B6-5x5-COR	0.041	0.014		
R – VI – T	Constant	59.148	0.000	0.492	7.678
	EVI	-1065.453	0.000		
	EVI2	1167.627	0.000		
	B3-7x7-M	0.387	0.007		
	B4-9x9_DIS	-0.151	0.000		
	B5-5x5-COR	-0.058	0.001		
	B5-9x9-M	-0.408	0.001		
	B5-9x9-HOM	-0.176	0.000		
	B6-5x5-COR	0.041	0.014		

of S_i; and m, number of compared models.

The model validation was based on the residuals between observed and predicted values for the validation data set, which included 34 sample plots as independent data. The null hypothesis of the mean of residual equals to zero was tested using the Student's t-test at the 95% probability level. If Student's t-tests show no significantly statistically differences and the mean residuals do not significantly differ from zero, it can be inferred that the derived regression models are statistically suitable for predicting the stand attributes using a Landsat 8 OLI satellite image variables in analyzing stand attributes of pure Scots pine plantation forests.

Table 5. Multiple Linear Regression Results for Stand Basal Area

Independent variable groups	Independent variables (X_i)	Coefficients (b_i)	p-value	R^2	SEE
R	Constant B5	75.587 -242.730	0.000 0.000	0.221	13.135
VI	Constant Albedo	71.215 -64.641	0.000 0.000	0.217	13.171
T	Constant B4-5x5-VAR B5-3x3-M B6-3x3-VAR B7-9x9-M	61.938 0.251 -0.188 -0.085 -0.204	0.000 0.000 0.010 0.029 0.001	0.316	12.498
R – VI	Constant B5	75.587 -242.730	0.000 0.000	0.221	13.135
R – T	Constant B5 B2-5x5-SM B3-3x3-ENT B4-3x3-VAR	59.915 -263.017 0.094 0.060 0.101	0.000 0.000 0.001 0.018 0.015	0.342	12.264
VI – T	Constant Albedo B2-9x9-SM B4-3x3-VAR B6-9x9-HOM	72.872 -67.363 0.161 0.116 -0.124	0.000 0.000 0.002 0.004 0.017	0.338	12.296
R – VI – T	Constant B5 B2-5x5-SM B3-3x3-ENT B4-3x3-VAR	59.915 -263.017 0.094 0.060 0.101	0.000 0.000 0.001 0.018 0.015	0.342	12.264

III. RESULTS AND DISCUSSION

Results

A multiple linear regression was used to estimate some stand attributes such as mean diameter, stand basal area, stand volume, number of trees, and stand density based on reflectance values, vegetation indices, and texture values obtained from the Landsat 8 OLI satellite image. The multiple linear regression techniques were utilized to determine the predictor remote sensing values for estimating stand attributes and linear regression models for each stand parameter. Using 6 reflectance values, 24 vegetation indices, and 192 texture values for candidate independent variable groups, all stand parameters were fitted. Values of the selected independent variables, their coefficients, *p* values of coefficients, and coefficients of determination (R^2) and standard errors (*SEE*) of the best regression models for each independent variable group were summarized in Tables 4, 5, 6, 7 and 8. Relative ranks of regression models were presented in Table 9.

Table 6. Multiple Linear Regression Results for Stand Volume

Independent variable groups	Independent variables (X_i)	Coefficients (b_i)	*p*-value	R^2	*SEE*
R	Constant	798.892	0.000	0.214	146.729
	B5	-2655.013	0.000		
VI	Constant	849.175	0.000	0.223	146.630
	Albedo	-490.283	0.003		
	EVI	-973.031	0.037		
T	Constant	684.523	0.000	0.341	137.206
	B4-5x5-VAR	2.293	0.000		
	B5-3x3-M	-2.606	0.002		
	B5-3x3-DIS	1.166	0.020		
	B6-7x7-VAR	-1.843	0.001		
	B7-9x9-M	-1.881	0.005		
R – VI	Constant	798.892	0.000	0.214	146.729
	B5	-2655.013	0.000		
R – T	Constant	798.892	0.000	0.214	146.729
	B5	-2655.013	0.000		
VI – T	Constant	713.698	0.000	0.276	142.297
	Albedo.	-1579.370	0.000		
	B6-3x3-M	5.817	0.001		
	B7-9x9-M	-2.395	0.013		
R – VI – T	Constant	798.892	0.000	0.214	146.729
	B5	-2655.013	0.000		

Table 7. Multiple Linear Regression Results for Number of Trees

Independent variable groups	Independent variables (X_i)	Coefficients (b_i)	*p*-value	R^2	*SEE*
T	Constant	1022.704	0.002	0.456	190.949
	B4-9x9-VAR	3.112	0.001		
	B5-3x3-M	10.069	0.000		
	B5-5x5-SM	5.437	0.000		
	B6-3x3-M	-21.956	0.000		
	B7-3x3-M	11.740	0.001		
R – T	Constant	1022.704	0.002	0.456	190.949
	B4-9x9-VAR	3.112	0.001		
	B5-3x3-M	10.069	0.000		
	B5-5x5-SM	5.437	0.000		
	B6-3x3-M	-21.956	0.000		
	B7-3x3-M	11.740	0.001		
VI – T	Constant	-977.840	0.000	0.534	177.746
	B4-9x9-CONT	4.507	0.000		
	B5-9x9-M	13.685	0.000		
	B5-9x9-HOM	4.224	0.000		
	B6-5x5-M	-9.972	0.000		
	B6-9x9-VAR	3.127	0.000		
	B6-9x9-COR	-0.837	0.041		
R – VI – T	Constant	-977.840	0.000	0.534	177.746
	B4-9x9-CONT	4.507	0.000		
	B5-9x9-M	13.685	0.000		
	B5-9x9-HOM	4.224	0.000		
	B6-5x5-M	-9.972	0.000		
	B6-9x9-VAR	3.127	0.000		
	B6-9x9-COR	-0.837	0.041		

Best regression results for each stand attributes were determined using the independent variable groups containing texture values. For the mean diameter, stand basal area, and number of trees, the most suitable regression models contained different combinations of vegetation indices and texture values. Although some of texture values were sufficient for the determination of best regression model of stand volume, the best stand density model included not only texture values of successful models for other stand properties, but also included reflectance values.

When the relative ranks of the regression models were compared for the mean diameter, the model. which includes vegetation indices and texture values, was considered as best, similar to the model containing all three groups of independent variables, although both models contained the same independent variables.

Thus, the model that includes vegetation indices and texture values was considered as the most suitable model for predicting stand attributes.

Table 9 shows eight, four, five, and six variables included in the best regression models of mean diameter, basal area, stand volume, number of trees, and stand density. respectively. All coefficients of these variables and constants of these models were statistically significant, suggesting that all stand parameters were fitted moderately with regression models. The highest R^2 value (R^2=0.534) was derived for estimating the number of trees, while lowest (R^2=0.338) for bsala area. The R^2 values of mean diameter, stand volume, and stand density models were more or less similar,

Table 8. Multiple Linear Regression Results for Stand Density

Independent variable groups	Independent variables (X_i)	Coefficients (b_i)	*p*-value	R^2	*SEE*
R	Constant B6	10.021 -34.673	0.000 0.000	0.229	2.103
VI	Constant ND73	9.177 -31.770	0.000 0.000	0.238	2.091
T	Constant B2-5x5-SM B3-5x5-ENT B4-3x3-VAR B7-3x3-M	2.624 0.017 0.014 0.025 -0.038	0.038 0.001 0.018 0.001 0.000	0.349	1.963
R – VI	Constant ND73	9.177 -31.770	0.000 0.000	0.238	2.091
R – T	Constant B6 B2-5x5-SM B3-5x5-ENT B4-3x3-VAR B4-3x3-SM B6-3x3-HOM	5.019 -32.791 0.017 0.017 0.016 0.014 -0.009	0.010 0.000 0.001 0.008 0.018 0.007 0.049	0.424	1.865
VI – T	Constant ND73 B2-9x9-SM B4-3x3-VAR B6-9x9-HOM	9.352 -33.659 0.029 0.020 -0.022	0.000 0.000 0.000 0.001 0.007	0.385	1.908
R – VI – T	Constant ND73 B2-9x9-SM B4-3x3-VAR B6-9x9-HOM	9.352 -33.659 0.029 0.020 -0.022	0.000 0.000 0.000 0.001 0.007	0.385	1.908

Table 9. Relative Ranks of Regression Models

Stand Attribute	Independent variable groups	Number of variables	R^2 (R_i)	*RMSE* (R_i)	*MAE* (R_i)	Total R_i	General rank
Mean diameter (d_q, cm)	R	3	0.186 (7.00)	9.3 (7.00)	7.1 (7.00)	21.00	7.00
	VI	2	0.204 (6.65)	9.2 (6.68)	7.0 (6.33)	19.66	6.55
	T	4	0.408 (2.65)	8.0 (2.89)	6.4 (2.33)	7.88	2.63
	R – VI	2	0.204 (6.65)	9.2 (6.68)	7.0 (6.33)	19.66	6.55
	R – T	6	0.433 (2.16)	7.8 (2.26)	6.2 (1.00)	5.42	1.81
	VI – T	8	0.492 (1.00)	7.4 (1.00)	6.2 (1.00)	3.00	1.00
	R – VI – T	8	0.492 (1.00)	7.4 (1.00)	6.2 (1.00)	3.00	1.00
Basal area (G, m^2 ha^{-1})	R	1	0.221 (6.81)	13.069 (6.80)	10.400 (7.00)	20.61	7.00
	VI	1	0.217 (7.00)	13.105 (7.00)	10.295 (6.37)	20.37	6.92
	T	4	0.316 (2.25)	12.245 (2.26)	9.497 (1.60)	6.11	1.95
	R – VI	1	0.221 (6.81)	13.069 (6.80)	10.400 (7.00)	20.61	7.00
	R – T	4	0.342 (1.00)	12.016 (1.00)	9.790 (3.35)	5.35	1.69
	VI – T	4	0.338 (1.19)	12.048 (1.18)	9.397 (1.00)	3.37	1.00
	R – VI – T	4	0.342 (1.00)	12.016 (1.00)	9.790 (3.35)	5.35	1.69
Stand volume (V, m^3 ha^{-1})	R	1	0.214 (7.00)	145.993 (7.00)	116.320 (7.00)	21.00	7.00
	VI	2	0.223 (6.57)	145.156 (6.59)	116.084 (6.82)	19.99	6.66
	T	5	0.341 (1.00)	133.732 (1.00)	108.309 (1.00)	3.00	1.00
	R – VI	1	0.214 (7.00)	145.993 (7.00)	116.320 (7.00)	21.00	7.00
	R – T	1	0.214 (7.00)	145.993 (7.00)	116.320 (7.00)	21.00	7.00
	VI – T	3	0.276 (4.07)	140.146 (4.14)	109.105 (1.60)	9.81	3.27
	R – VI – T	1	0.214 (7.00)	145.993 (7.00)	116.320 (7.00)	21.00	7.00
Number of trees (N, per ha)	T	5	0.456 (4.00)	186.1 (4.00)	143.8 (4.00)	12.00	4.00
	R – T	5	0.456 (4.00)	186.1 (4.00)	143.8 (4.00)	12.00	4.00
	VI – T	6	0.534 (1.00)	172.3 (1.00)	137.6 (1.00)	3.00	1.00
	R – VI – T	6	0.534 (1.00)	172.3 (1.00)	137.6 (1.00)	3.00	1.00
Stand density (SD)	R	1	0.229 (7.00)	2.09 (7.00)	1.60 (7.00)	21.00	7.00
	VI	1	0.238 (6.72)	2.08 (6.79)	1.60 (7.00)	20.51	6.84
	T	4	0.349 (3.31)	1.92 (3.36)	1.45 (2.50)	9.16	3.05
	R – VI	1	0.238 (6.72)	2.08 (6.79)	1.60 (7.00)	20.51	6.84
	R – T	6	0.424 (1.00)	1.81 (1.00)	1.40 (1.00)	3.00	1.00
	VI – T	4	0.385 (2.20)	1.87 (2.29)	1.40 (1.00)	5.49	1.83
	R – VI – T	4	0.385 (2.20)	1.87 (2.29)	1.40 (1.00)	5.49	1.83

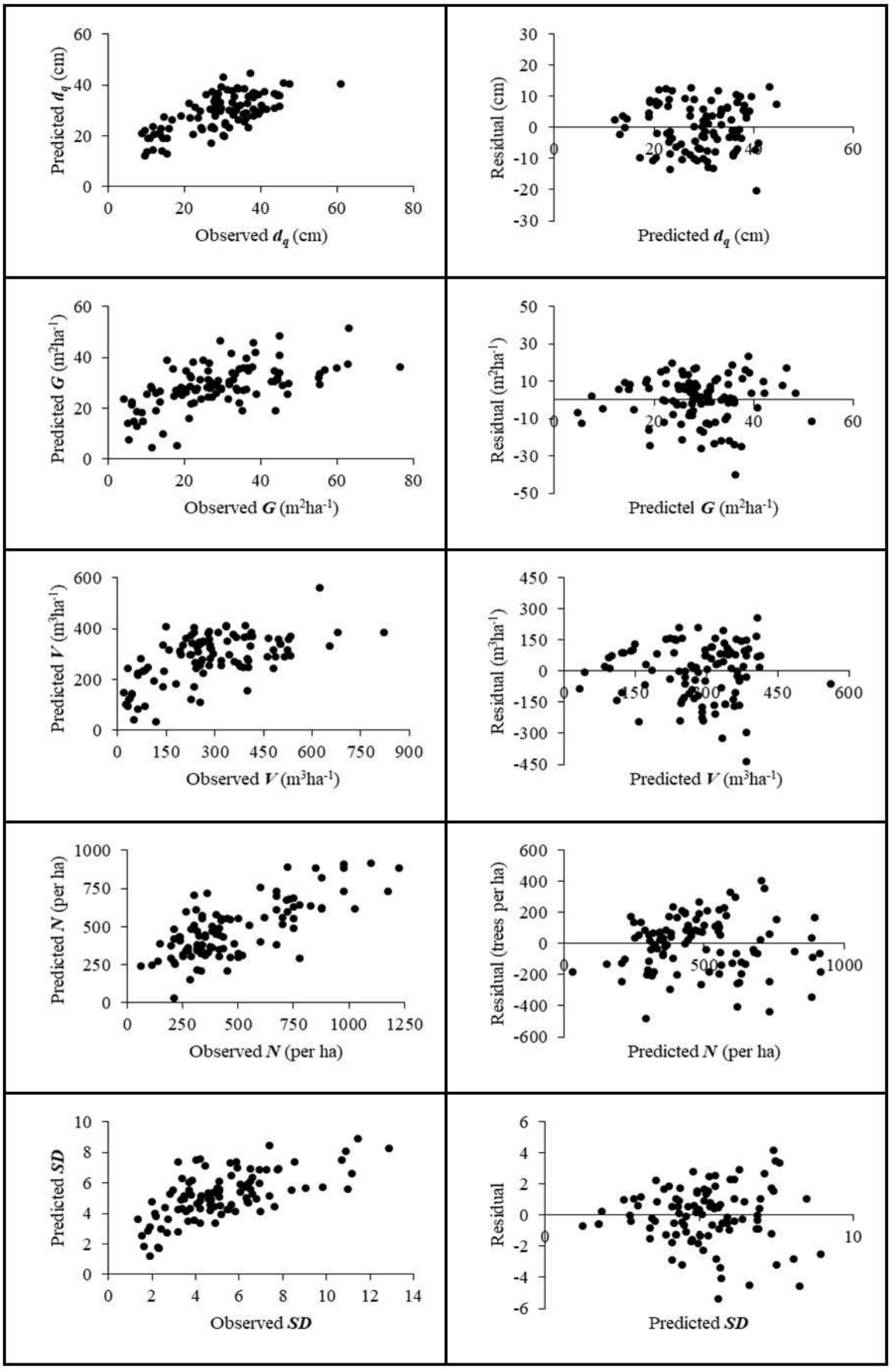
Predicted d_q (cm)
Observed d_q (cm)
Residual (cm)
Predicted d_q (cm)
Predicted G (m²ha⁻¹)
Observed G (m²ha⁻¹)
Residual (m²ha⁻¹)
Predictel G (m²ha⁻¹)
Predicted V (m³ha⁻¹)
Observed V (m³ha⁻¹)
Residual (m³ha⁻¹)
Predicted V (m³ha⁻¹)
Predicted N (per ha)
Observed N (per ha)
Residual (trees per ha)
Predicted N (per ha)
Predicted SD
Observed SD
Residual
Predicted SD

with R^2 values of 0.492, 0.341, and 0.424, respectively. The validity of the best regression models were determined using a Student's *t*-test using the validation data obtained from 34 sample plots. For all models, the observed and predicted values showed no significant differences ($p>0.05$), suggesting the usability of derived models.

The observed vs. predicted values and residual distributions of predicted stand attributes using all data from 135 sample plots are shown in Figure 3. When the residual distributions were examined, it can be observed that the residuals were distributed randomly, and the mean residuals were close to zero. Mean residuals for d_q, *G*, *V*, *N* and *SD* estimates were -0.4 cm, -0.452 m^2 ha^{-1}, -3.010 m^3 ha^{-1}, 24.3 trees per ha, and 0.06 for the best regression models, respectively.

Discussion

There are some studies to estimate stand parameters using Landsat satellite images, in which the reflectance values and vegetation indices [3]. Kahriman *et al.* [23] and Günlü & Kadıoğulları [13] and texture values [40], were used as independent variables. Texture values obtained from the other satellite data images were also used in other studies for estimating stand parameters, such as SPOT-5 [5, 45], WorldView-2 [36] and RapidEye [44].

Other regression model that utilized band values of Landsat ETM+ image [13] had lower prediction success (R^2=0.250) for mean diameter of *Pinus brutia* and *Pinus nigra* stands in the Western Türkiye than the model developed in this study (R^2=0.492). Similarly, the model using texture values obtained from Landsat 8 OLI for mean diameter of *Pinus nigra* stands in the Northern Türkiye had also lower R^2 values as 0.399 [40]. Wallner *et al.* [44] stated that the mean diameter of mixed *Picea abies*, *Fagus sylvatica,* and *Abies alba* forests of Bavaria region of Germany could be estimated with higher success using a RapidEye satellite image data (R^2=0.550).

For stand basal area models using various types of Landsat image, Günlü & Kadıoğulları [13] and Sakici & Günlü [40] reported

R^2=0.320 and R^2=0.337, respectively, which are more or less similar to the observed values (R^2=0.338) in this study. The regression models based on the satellite data obtained from SPOT-5, WorldView-2, and RapidEye showed higher R^2 values for basal area estimates, ranging from 0.540 to 0.778 [5, 36, 44, 45]. The reported R^2 values in the studies of Mohammadi *et al*. [33], Günlü & Kadıoğulları [13], and Sakici & Günlü [40], which used texture values of Landsat satellites for stand volume estimation (R^2=0.430, R^2=0.370 and R^2=0.332, respectively) complemented the findings in this study (R^2=0.341). In contrast, models for SPOT-5. WorldView-2 and RapidEye images had higher R^2 values ranging from 0.420 to 0.820 for stand volume estimates [5, 36, 44, 45] than what were observed in this study. The reason why these studies obtained better results than ours may be due to the higher resolution of the satellite images used, the different stand structure, topography, etc. Other studies using Landsat ETM+ [33, 13] and Landsat TM [23] had various prediction successes with R^2 values between 0.440 and 0.734. Finally, the number of tree models using the data from other satellites had lower predictive reliability with R^2 values of 0.38 for WorldView-2 [36] and 0.40 for RapidEye [44].

IV. CONCLUSION AND RECOMMENDATIONS

Based on this study, the images generated by Landsat 8 OLI images could be used to predict some stand attributes of Scots Pine forest, although the predictive power vary from low to moderately strong, as indicated by the R^2 values of 0.492, 0.338, 0.341, 0.534, and 0.424, for the mean diameter, basal area, stand volume, number of trees, and stand density, respectively. While the prediction values of the mean diameter and number of trees models could be considered moderately good, the other models for basal area, stand volume, and stand density have shown lower prediction powers, which could be attributed to the low spatial resolution of the satellite image used, acquisition time, and correction errors of the satellite image, fitting method, stand and structures of the study area. Satellite images with high spatial resolution could be used and other fitting approaches such as machine learning methods could be conducted to improve the pre-

dictive power of these models. If the cost of satellite imagery is a problem, Sentinel 2 satellite images can be used because of better resolution than Landsat 8 OLI, and could be obtained free of charge.

V. ACKNOWLEDGEMENT

The authors would like to thank Head of Forest Management and Planning Department. General Directorate of Forestry, Türkiye for their support.

V. REFERENCES

[1] Abedi, R., Bonyad, A. E., Moridani, A. Y. & Shahbahrami. A. (2018). Evaluation of IRS and Landsat 8 OLI imagery data for estimation forest attributes using k nearest neighbour non-parametric method. *International Journal of Image and Data Fusion*, 9(4), 287-301.

[2] Bettinger, P., Boston, K., Siry, J., & Grebner, D. (2016). *Forest Management and Planning*. Academic Press.

[3] Blackburn, G. A. (1998). Spectral indices for estimating photosynthetic pigment concentrations: A test using senescent tree leaves. *International Journal of Remote Sensing*, *19*(4), 657-675.

[4] Blinn, C. E., House, M. N., Wynne, R. H., Thomas, V. A., Fox, T. R., & Sumnall. M. (2019). Landsat 8 based leaf area index estimation in loblolly pine plantations. *Forests*, *10*(3), 222.

[5] Castillo-Santiago, M. A., Ricker. M., & de Jong, B. H. (2010). Estimation of tropical forest structure from SPOT-5 satellite images. *International Journal of Remote Sensing*, *31*(10), 2767-2782.

[6] Chen, J. M. (1996). Evaluation of vegetation indices and a modified simple ratio for boreal applications. *Canadian Journal of Remote Sensing*, *22*(3), 229-242.

[7] Cohen, W. B., Spies, T. A., & Fiorella, M. (1995). Estimating the age and structure of forests in a multi-ownership landscape of western Oregon. USA. *International Journal of Remote Sensing*, *16* (4), 721-746.

[8] Crippen, R. E. (1990). Calculating the vegetation index fast-

er. *Remote Sensing of Environment*, *34*(1), 71-73.

[9] Curtis, R.O., Clendenen, G.W., & Demars, D.J. (1981). *A new Stand Simulator for Coastal Douglas-fir: DFSIM User's Guide*. U.S.D.A. Forest Service General Technical Report PNW-1128.

[10] Dube, T., Pandit, S., Shoko, C., Ramoelo, A., Mazvimavi, D., & Dalu. T. (2019). Numerical assessments of leaf area index in tropical savanna rangelands. South Africa using Landsat 8 OLI derived metrics and in-situ measurements. *Remote Sensing*, *11*(7), 829.

[11] Gitelson, A. A., Kaufman, Y. J., & Merzlyak, M. N. (1996). Use of a green channel in remote sensing of global vegetation from EOS-MODIS. *Remote Sensing of Environment*, *58*(3), 289-298.

[12] Goel, N. S., & Qin, W. (1994). Influences of canopy architecture on relationships between various vegetation indices and LAI and FPAR: A computer simulation. *Remote Sensing Reviews*, *10* (4), 309-347.

[13] Günlü, A. & Kadıoğulları, A. İ. (2018). Modeling forest stand attributes using Landsat ETM+ and QuickBird satellite images in western Turkey. *Bosque*, *39*(1), 49-60.

[14] Günlü, A., Keleş, S., Ercanli, İ., & Şenyurt, M. (2021). Estimation of aboveground stand carbon using Landsat 8 OLI satellite image: A case study from Turkey. In *Spatial Modeling in Forest Resources Management* (pp. 385-403), Springer, Cham.

[15] Haralick, R. M., Shanmugam, K., & Dinstein, I. H. (1973). Textural features for image classification. *IEEE Transactions on Systems. Man. and Cybernetics*, *6*, 610-621.

[16] Hardisky, M.A., Klemas, V., & Smart, R. (1983). The influence of soil salinity. growth form. and leaf moisture on the spectral radiance of *Spartina alterniflora* canopies. *Photogrammetric Engineering and Remote Sensing*, *49*, 77 – 83.

[17] Holmgren, P., & Thuresson, T. (1998). Satellite remote sensing for forestry planning – a review. *Scandinavian Journal of Forest Research*, *13*(1-4), 90-110.

[18] Huete, A. R. (1988). A soil-adjusted vegetation index (SAVI). *Remote Sensing of Environment*, *25*(3), 295-309.

[19] Hunt. E. R.. & Rock. B. N. (1989). Detection of changes in leaf water content using near-and middle-infrared reflectances. *Remote Sensing of Environment*, *30*(1), 43-54.

[20] Izadi, S., & Sohrabi, H. (2020). Estimating the spatial distribution of above-ground carbon of Zagros Forests using regression kriging, geographically weighted regression kriging and Landsat 8 imagery. *Journal of Environmental Science and Technology*, 24(3), 17-30.

[21] Jiang, Z., Huete, A. R., Didan, K., & Miura, T. (2008). Development of a two-band enhanced vegetation index without a blue band. *Remote Sensing of Environment*, *112*(10), 3833-3845.

[22] Jordan, C. F. (1969). Derivation of leaf-area index from quality of light on the forest floor. *Ecology*, *50*(4), 663-666.

[23] Kahriman, A., Günlü, A., & Karahalil, U. (2014). Estimation of crown closure and tree density using Landsat TM satellite images in mixed forest stands. *Journal of the Indian Society of Remote Sensing*, *42*(3), 559-567.

[24] Kaptan, S., Aksoy, H., & Durkaya, B. (2020). Estimation of uneven-aged forest stand parameters, crown closure and land use/cover using the Landsat 8 OLI satellite image. *Geocarto International*, 37(5), 1408-1425.

[25] Kaufman, Y. J., & Remer, L. A. (1994). Detection of forests using mid-IR reflectance: An application for aerosol studies. *IEEE Transactions on Geoscience and Remote Sensing*, *32*(3), 672-683.

[26] Kaufman, Y. J., & Tanre, D. (1992). Atmospherically resistant vegetation index (ARVI) for EOS-MODIS. *IEEE Transactions on Geoscience and Remote Sensing*, *30*(2), 261-270.

[27] Key, C., & Benson, N. C. (2006). *Landscape assessment: sampling and analysis methods.* USDA Forest Service. Rocky Mountain Research Station General Technical Report. RMRS-GTR -164-CD.

[29] Liu, H. Q., & Huete, A. (1995). A feedback based modification of the NDVI to minimize canopy background and atmospheric noise. *IEEE Transactions on Geoscience and Remote Sensing*, *33* (2), 457-465.

[30] Lu, D., Mausel, P., Brondizio, E., & Moran, E. (2004). Rela-

tionships between forest stand parameters and Landsat TM spectral responses in the Brazilian Amazon Basin. *Forest Ecology and Management*, *198 (1*-149-167.

[31] Luo, K., Wei, Y., Du, J., Liu, L., Luo, X., Shi, Y., Pei, X., Lei, N., Song, C., Li, J., & Tang, X. (2021). Machine learning-based estimates of aboveground biomass of subalpine forests using Landsat 8 OLI and Sentinel-2B images in the Jiuzhaigou National Nature Reserve. Eastern Tibet Plateau. *Journal of Forestry Research*, 33(4), 1329-1340.

[32] McFeeters, S. K. (1996). The use of the Normalized Difference Water Index (NDWI) in the delineation of open water features. *International Journal of Remote Sensing*, *17*(7), 1425-1432.

[33] Mohammadi, J., Shataee Joibary, S., Yaghmaee, F., & Mahiny, A. S. (2010). Modelling forest stand volume and tree density using Landsat ETM+ data. *International Journal of Remote Sensing*, *31*(11), 2959-2975.

[34] Nasution, A. A., Muslih, A. M., Ar-Rasyid, U. H., & Anhar, A. (2022). Land cover classification using Landsat 8 OLI in West Langsa Sub district. Langsa City. In *IOP Conference Series: Earth and Environmental Science* (Vol. 951. No. 1. p. 012080). IOP Publishing.

[35] Ou, G., Li, C., Lv, Y., Wei, A., Xiong, H., Xu, H., & Wang, G. (2019). Improving aboveground biomass estimation of *Pinus densata* forests in Yunnan using Landsat 8 imagery by incorporating age dummy variable and method comparison. *Remote Sensing*, *11*(7), 738.

[36] Ozdemir, I., & Karnieli, A. (2011). Predicting forest structural parameters using the image texture derived from WorldView -2 multispectral imagery in a dryland forest. Israel. *International Journal of Applied Earth Observation and Geoinformation*, *13*(5), 701 -710.

[37] Qi, J., Chehbouni, A., Huete, A. R., Kerr, Y. H., & Sorooshian, S. (1994). A modified soil adjusted vegetation index. *Remote Sensing of Environment*, *48*(2), 119-126.

[38] Poudel, K. P., & Cao, Q. V. (2013). Evaluation of methods to predict Weibull parameters for characterizing diameter distributions. *Forest Science*, *59*(2), 243-252.

[39] Rouse, J.W., Hass, R.H., Shell, J.A. & Deering, D.W. (1974). Monitoring vegetation systems in the Great Plains with ERTS-l. Proceedings, *3rd Earth Resources Technology Satellite Symposium*, 1: 309-317.

[40] Sakici, O. E., & Günlü, A. (2018). Artificial intelligence applications for predicting some stand attributes using Landsat 8 OLI Satellite data: A case study from Turkey. *Applied Ecology and Environmental Research*, 16(4), 5269–5285.

[41] Soudani, K., Hmimina, G., Dufrêne, E., Berveiller, D., Delpierre, N., Ourcival, J. M., Rambal, S., & Joffre, R. (2014). Relationships between photochemical reflectance index and light-use efficiency in deciduous and evergreen broadleaf forests. *Remote Sensing of Environment*, *144*, 73-84.

[42] Tucker, C. J. (1980). A spectral method for determining the percentage of green herbage material in clipped samples. *Remote Sensing of Environment*, *9*(2), 175-181.

[43] Turgut, R., & Günlü, A. (2020). Estimating aboveground biomass using Landsat 8 OLI satellite image in pure Crimean pine (*Pinus nigra* JF Arnold subsp. *pallasiana* (Lamb.) Holmboe) stands: a case from Turkey. *Geocarto International*, 37(3), 720-734.

[44] Wallner, A., Elatawneh, A., Schneider, T., & Knoke, T. (2015). Estimation of forest structural information using RapidEye satellite data. *Forestry: An International Journal of Forest Research*, *88*(1), 96-107.

[45] Xie, S., Wang, W., Liu, Q., Meng, J., Zhao, T., & Huang, G. (2017). Estimation of forest stand parameters using SPOT-5 satellite images and topographic information. *Preprints*, 2017100017.

[46] Yavuz, H., Mısır, N., Mısır, M., Tüfekçioğlu, A., Sarıyıldız, T., Kara, Ö., Altun, L., Yılmaz, M., Sakıcı, O.E., Karahalil, U., Ercanlı, İ., Kahriman, A., Küçük, M., Bolat, İ., Bayburtlu, Ş., Bilgili, F., & Meydan, G. (2010). Karadeniz Bölgesi Saf ve Karışık Sarıçam (*Pinus sylvestris* L.) Meşcereleri İçin Mekanistik Büyüme Modellerinin Geliştirilmesi. Biyokütle ve Karbon Depolama Miktarlarının Belirlenmesi. TÜBİTAK Araştırma (1001) Projesi. Proje No: 106O274.